Risk and reward: explosive eruptions and obsidian lithic resource at Nabro volcano (Eritrea)

Clive Oppenheimer[1,2], Lamya Khalidi[3], Bernard Gratuze[4], Nels Iverson[5], Christine Lane[1], Céline Vidal[1], Yonatan Sahle[6], Nick Blegen[1], Ermias Yohannes[7], Amy Donovan[1], Berhe Goitom[8], James O.S. Hammond[9], Edward Keall[10], Ghebrebrhan Ogubazghi[11], Bill McIntosh[5], Ulf Büntgen[1,12,13]

[1]Department of Geography, University of Cambridge, Downing Place, Cambridge CB2 3EN, UK. co200@cam.ac.uk, corresponding author [Lane: csl44@cam.ac.uk ; Vidal: cv325@cam.ac.uk ; Donovan: ard31@cam.ac.uk ; Blegen: nb599@cam.ac.uk ; Büntgen: ulf.buentgen@geog.cam.ac.uk]
[2]McDonald Institute for Archaeological Research, Downing Street, Cambridge, CB2 3ER, UK.
[3]UMR 7264—Centre Nationale de la Recherche Scientifique—Culture et Environnements Préhistoire, Antiquité, Moyen Âge (CEPAM)/Univ. Côte d'Azur, 24 avenue des Diables Bleus, Nice 06357, France. Lamya.KHALIDI@cepam.cnrs.fr
[4]IRAMAT-CEB, UMR5060, CNRS/Université d'Orléans, Orléans, France. gratuze@cnrs-orleans.fr
[5]New Mexico Bureau of Geology and Mineral Resources & Department of Environmental Science, New Mexico Institute of Mining and Technology, Socorro, NM 87801, USA. nels.iverson@nmt.edu [McIntosh: mcintosh@nmt.edu]
[6]DFG Center for Advanced Studies: 'Words, Bones, Genes, Tools', University of Tübingen, Rümelinstraße 23, 72070 Tübingen, Germany. yonatan.sahle@ifu.uni-tuebingen.de
[7]Department of Mines, Eritrea Geological Surveys, PO Box 272, Asmara, Eritrea, ermias_yohannes@yahoo.com
[8]School of Earth Sciences, University of Bristol, Queens Road, Bristol BS8 1RJ, UK. berhe.goitom.gezahegn@bristol.ac.uk
[9]Department of Earth and Planetary Sciences, Birkbeck College, University of London, London WC1E 7HX, UK. james.hammond@bbk.ac.uk
[10]Royal Ontario Museum, University of Toronto, 100 Queen's Park, Toronto, ON, M5S 2C6, Canada, edk@rom.on.ca
[11]Department of Earth Sciences, Eritrea Institute of Technology, PO Box 12676, Asmara, Eritrea [ogubazghi_ghebrebrhan@yahoo.com]
[12]Swiss Federal Research Institute (WSL), 8903 Birmensdorf, Switzerland.
[13]Global Change Research Centre (CzechGlobe), 603 00 Brno, Czech Republic

Abstract

Compared with other manifestations of climate variability that may not be perceived within a human lifetime, abrupt environmental disturbances arising from volcanism can be directly experienced. Despite abundant Pleistocene calderas in the East African Rift and Afar, and the significance of regional tephra horizons for archaeological and paleoenvironmental dating, the entanglements of volcanoes and their eruptions with human behaviour and paleoecology have received little attention. Here, we focus on the intertwined human and eruptive history at Nabro, a caldera-topped volcanic massif close to the Red Sea littoral of Eritrea. Nabro exemplifies the antagonism of

opportunities and threats posed by a large silicic volcano, active at least since the Middle Pleistocene and as recently as 2011. Using argon isotopic measurements, we establish the first chronology of key eruptive stages of Nabro and neighbouring Mallahle revealing a history of explosive and effusive volcanism in the Middle and Late Pleistocene. Past eruptions were an important source of obsidian that was exchanged over long distances across land and sea during the Neolithic. We infer that the availability of high-quality obsidian, combined with Nabro's favourable microclimate and proximity to the Red Sea coast, likely attracted humans to this volcanic landmark since the later Middle Pleistocene. Drawing on observations of the immediate impact of the 2011 eruption on landscape and local pastoralist communities, we consider the impacts of past volcanic cataclysms on human populations. In addition to the threat to life, explosive eruptions of Nabro circa 130 ka and 62 ka ago would have abruptly curtailed procurement of its obsidian resource. Our findings suggest further attention be paid to evaluating the significance of East African volcanic landscapes, eruptions and resources for understanding human behaviour in deep antiquity.

Keywords: Late Quaternary; Geoarchaeology; East Africa; Ar-Ar geochronology; obsidian geochemistry

1. Introduction

The biogeography and paleohydrology of the East African Rift (EAR) and Afar provided important evolutionary stimuli for the lineages of modern humans and our extinct hominin relatives (King & Bailey, 2006; Kingston, 2007; Trauth et al., 2010; Bailey & King, 2011). Patterns of occupation and migration were likely influenced by landscape dynamics of the EAR and its proximity to the Red Sea and Gulf of Aden (Walter et al., 2000; Oppenheimer, 2009; Bailey & King, 2011). Despite abundant interdisciplinary research on the role of climate-driven environmental factors in human biological and behavioural evolution (e.g., Maslin et al., 2014), few works have considered the significance of volcanism for prehistoric populations and the landscapes and resources they depended on (e.g., Basell, 2008; Oppenheimer, 2011). The largest explosive eruptions, which in Ethiopia appear to cluster temporally in the Middle and Late Pleistocene (Hutchison et al., 2016), covered wide areas with thick tephra deposits, triggering abrupt and profound ecosystem disturbance by sterilizing the

land surface and changing local hydrology. Such effects and the subsequent ecological successions have been well documented following several historical eruptions, including those of Krakatau in 1883 (e.g., Whittaker et al., 1989), Surtsey in the mid-1960s (e.g., del Moral & Magnússon, 2014), and Mount St. Helens in 1980 (e.g., Dale et al., 2005). However, we are unaware of comparable studies carried out in the EAR or Afar.

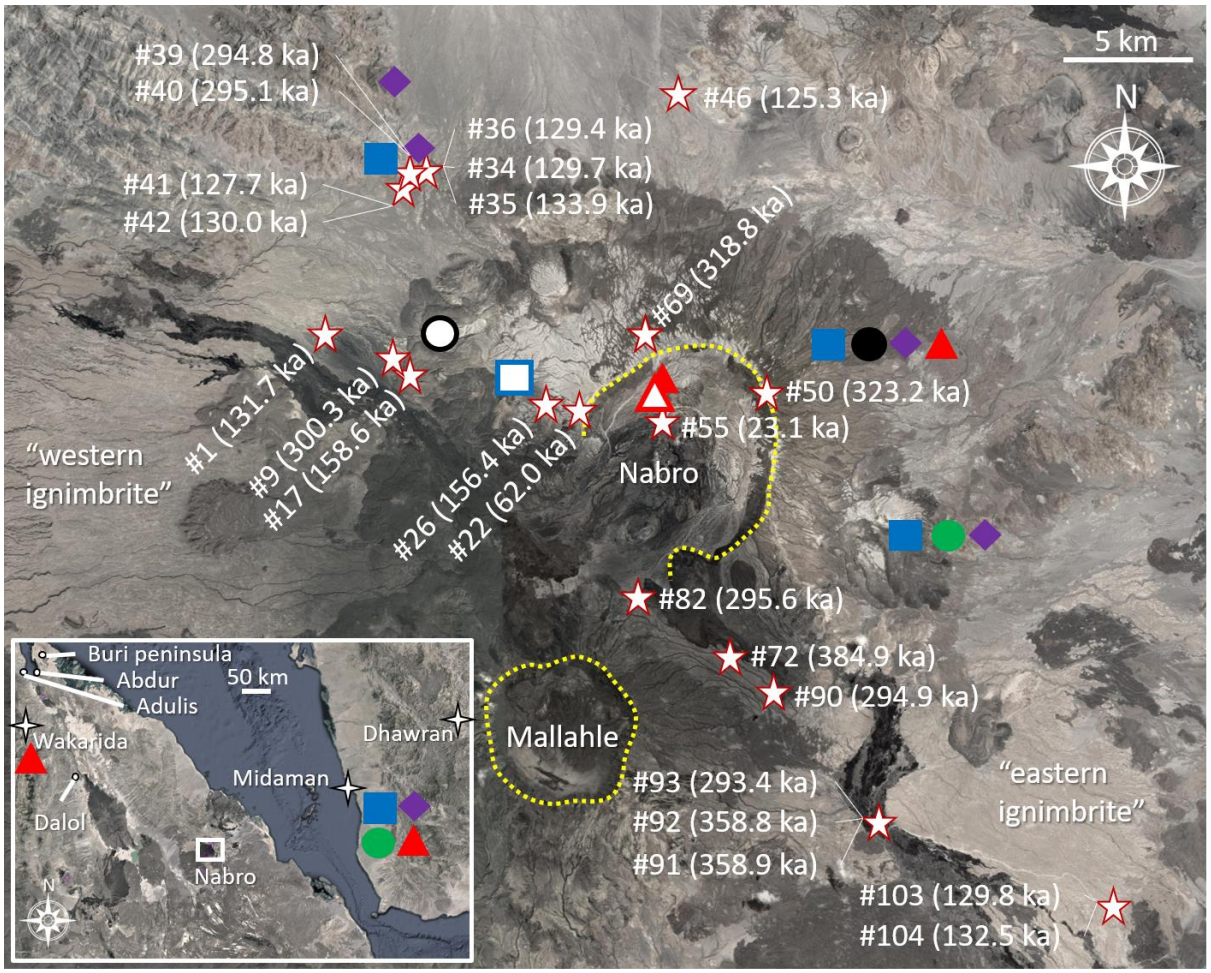

Fig. 1. Satellite image of Nabro and Mallahle (caldera outlines in dashed-yellow outline) overlaid with locations of lava, pyroclastic and obsidian lithic samples. Red and white stars represent specimens that were dated by the argon-argon method, with sample number (which can be cross-referenced with Table 1) and age as given. Open square, circle and triangle indicate obsidian source locations (UNWF, LNWF and IC, respectively) with shape and rim colour matching obsidian lithic populations as shown (coloured symbols as in Fig. 8); note that group 2 and 4 lithics do not directly match any of the analysed source rocks). Regional map (inset) of Southern Red Sea shows other locations discussed in

the text, and indicates geochemical affinities of obsidian lithics from al-Midaman in Yemen and Wakarida in Ethiopia. Base images from Google Earth.

The Southern Red Sea Region of Eritrea is considered critical for understanding Late Pleistocene human adaptation to, and migration across, costal landscapes, as well as contact between Africa and Arabia (Oppenheimer, 2009; 2012; Rose et al., 2013). As a segment of the hypothesised 'southern route' of modern human dispersal beyond Africa, the Eritrean littoral may have served as both refugium and corridor (e.g., Lahr & Foley, 1994; Bailey et al., 2008; Beyin, 2011a; Al-Abri et al., 2012; Armitage et al., 2011). Populations expanded through the Holocene, and the region is key also to understanding the trajectory seen in eastern Africa from hunter-gatherers to settled pastoralists (Lesur-Gebremariam , 2009; Lesur 2014; Coudert et al., 2018) and to coastal fishing and foraging settlements that were linked to the natural resources of both the Arabian shores and Ethiopian highlands (Khalidi, 2009; Khalidi et al. 2018). Despite its interdisciplinary nexus, there has been only limited work on Eritrea's late prehistoric archaeology.

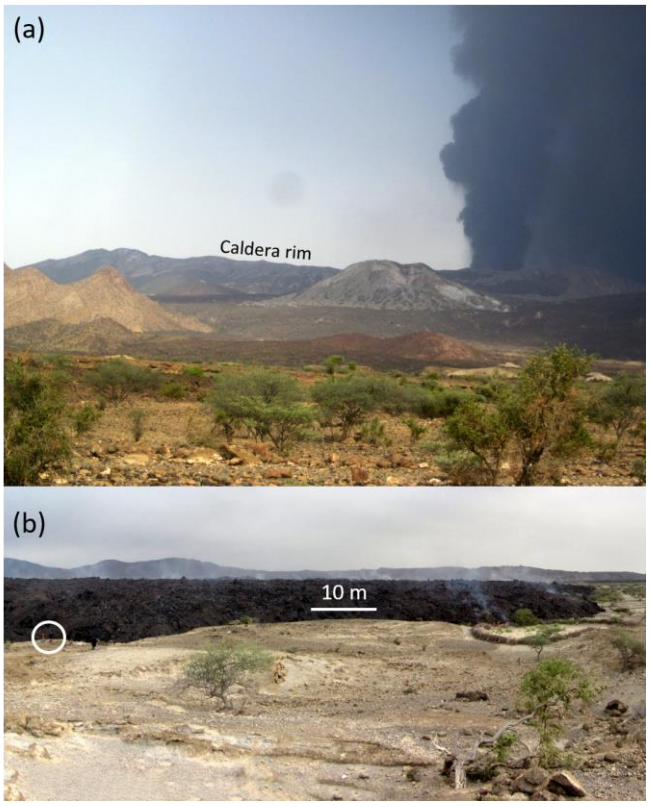

Fig. 2. Photographs of (a) the ash cloud (looking to the south-east from a distance of about 10 km to the caldera rim; visible part of the ash cloud here rises approximately 2–3 km), and (b) active lava

flow front at Nabro on 22 June 2011 (figures, within the white circle, give a sense of scale). Note the small kraal *being consumed in (b). Courtesy of Seife Berhe.*

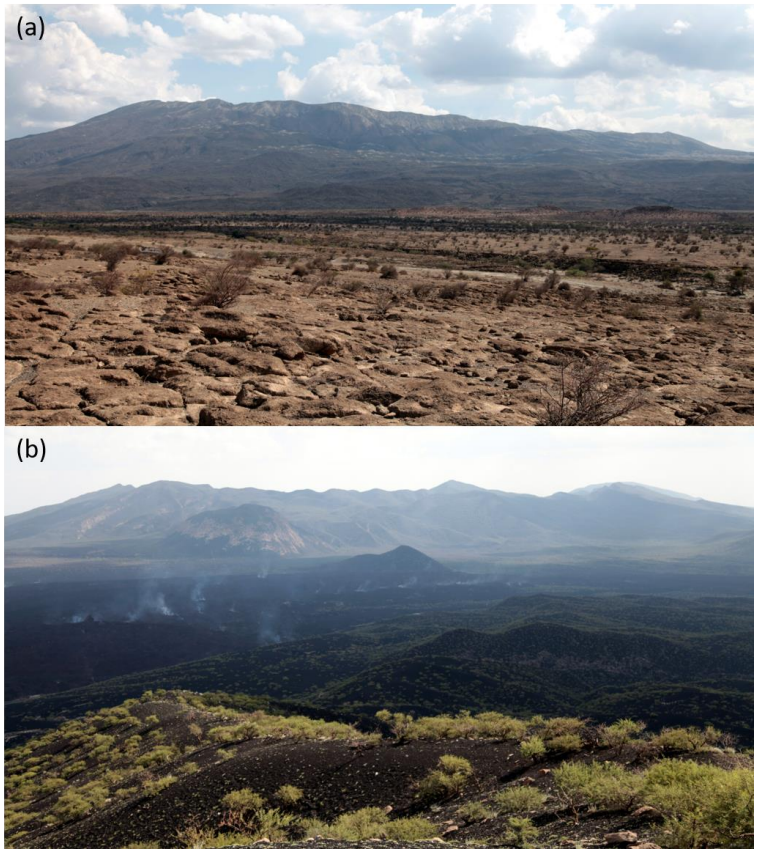

Fig. 3. Photographs of (a) Nabro seen from the east and a distance of approximately 9 km (130 ka ignimbrite forms the platform in the foreground; note also lighter-coloured areas close to the caldera rim, which are 62 ka tephra fall deposits; horizontal distance between opposing crests of the caldera is about 6.5 km), and (b) Mallahle, seen from west rim of Nabro caldera and looking approximately southwest across the flow field (seen smoking) from the 2011 eruption. Distance to caldera rims are about 8.5 km, and horizontal distance between opposing crests of the caldera is about 4 km. Dark material in foreground and covering Mallahle's slopes is 2011 tephra fallout.

The region also hosts several silicic volcanoes that have been little studied. One of the landmark volcanoes in Eritrea is the 2218-metre-high Nabro. Situated about 300 km southeast of the Aksumite port city of Adulis, and 200 km northwest of the Bab-el-Mandab strait (Wiart & Oppenheimer, 2005), it dominates a SSW-NNE trending volcanic range that rises above the predominantly basaltic lava plains of the Danakil desert (Fig. 1). Nabro erupted for the first time in recorded history in 2011 (Fig.

2; Goitom et al., 2015; Donovan et al., 2018; Hamlyn et al., 2018). Despite the generally sparse population in this region, the eruption displaced around 12,000 people, many of whom had been living within Nabro's caldera. During the eruption, a large quantity of sulfur dioxide was released to the atmosphere, generating aerosol capable of affecting the Earth's climate system (Ge et al., 2016). From geological and geomorphological perspectives, Nabro is notable for its approximately seven-kilometre-wide summit caldera, which opens towards the southwest, and for the wide apron of silicic ignimbrites that surrounds it. Immediately adjacent to Nabro is Mallahle volcano whose caldera is more than 5 km across (Fig. 3). It was also settled prior to the 2011 Nabro eruption and received substantial tephra fallout during that episode (Goitom et al., 2015). The presence of communities within both calderas, and their evacuation in 2011, hint at a much deeper history of resource exploitation, occupation and abandonment of Nabro and its neighbour.

1.1. Obsidian

Obsidian was an important resource in East Africa in the Middle Stone Age (MSA, Blegen, 2017), Later Stone Age (LSA, Ménard et al., 2014) and Neolithic (Gutherz et al., 2015; Khalidi et al. 2018). Obsidian is associated predominantly with silicic volcanoes. Outcrops are comparatively rare in the Danakil, where most of the volcanic products are basaltic in composition (Barberi et al., 1972). Obsidian tools and source rocks yield an exceptional means to track human mobility, interaction and exchange systems (Khalidi, 2009; Ambrose, 2012; Kuzmin et al., 2019). Obsidian eruption ages can also provide maximum ages for archaeological materials and sites (Morgan et al., 2009). Significant finds of obsidian tools from Eritrea include MSA flakes and blades in a circa 125 ka reef limestone terrace at Abdur (Walter et al., 2000; see also Sahle & Beyin, 2017, for survey of equivalent deposits near Dalol in northern Afar, Ethiopia), and an abundance of LSA lithics from Early and Middle Holocene sites on the Buri peninsula, just inland from Abdur (Beyin, 2011b). Availability of obsidian was likely a stimulus for maritime interaction along and across the Red Sea as early as the 6th millennium BCE (Khalidi, 2009), nourishing the growth of trading ports such as Adulis (Munro-Hay, 1982; Raunig, 2004). More broadly, obsidian exploitation is thought to have stimulated early human occupation, technological innovation (e.g., lithic manufacture and maritime and terrestrial

transport), variability in lithic repertoires between regions, and cultural innovation and interaction (Khalidi et al., 2010; Dumitru and Harrower, 2018).

The 2011 eruption of Nabro provided the first opportunity to undertake international fieldwork in this restricted area for more than a decade. In the course of undertaking these investigations (Goitom et al., 2015), surface scatters of obsidian cores, flakes, blades and *débitage* were observed (Fig. 4). Rhyolitic lava outcrops consisting of pristine obsidian were also noted, suggesting a likely primary raw material source for lithic production. These observations, combined with new geochronometry (reported here), stimulated us to consider the wider significance of Nabro volcano within the prehistoric social landscape. Accordingly, our aims here are to integrate studies of the obsidian artefacts and of the eruptive history of Nabro and Mallahle, and thereby to evaluate the intertwined histories of volcanism and humans in this region. We report the techno-typological evaluation of the lithic assemblage, and classify the geological and archaeological obsidians on the basis of their geochemistry, permitting the intercomparison of our lithics and outcrop samples as well as a search for geochemical matches with obsidian lithics found elsewhere in the Red Sea region (from littoral to plateaux).

Fig. 4. Photographs taken on the east flank of Nabro showing scatter of débitage *on the surface of the 130 ka ignimbrite.*

2. Materials and methods

2.1. Fieldwork

International fieldwork in Eritrea has been hampered since the war with Ethiopia that began in 1998, and the conflict was only formally ended in 2018. However, the 2011 eruption of Nabro provided an opportunity for two small-scale geological and seismological field missions to take place in October 2011 and 2012. The primary objectives were to understand the causes and nature of the eruption and to situate the event within the broader context of regional extensional tectonics. A small network of seismometers was installed to record post-eruptive seismicity (Hammond et al., 2011), and samples of the recently-erupted lava and tephra were collected (Donovan et al., 2018). The two expeditions also afforded an opportunity to sample older units of the volcanic stratigraphy, which had hitherto only been examined using satellite remote sensing data (Wiart & Oppenheimer, 2005). Notably, we reconnoitred and sampled ignimbrites found beyond the northern, eastern and southern flanks of Nabro; a pumiceous fall deposit that drapes parts of the caldera rim and upper flanks of the edifice (Fig. 1); and other prominent lavas and tephra deposits. We could not access areas across the border in Ethiopia but consider that some of the units sampled in Eritrea may originate from Mallahle volcano (Fig. 1, 3b).

Fig. 5. Primary source of obsidian outcropping on the northwest flank of Nabro (corresponds to geochemical group LNWF). We loosely associate this flow with the circa 257 ka rhyolitic lavas on the northwest flank.

While hiking across the terrain, we noticed an abundance of obsidian lithics at the surface (Fig. 4) and made a small collection of these, with most specimens found on the northwest, east and southeast sectors of the volcano and within the caldera; Fig. 1, 3a). While traversing the northwest flank of the volcano, we also observed and sampled outcrops of high-quality obsidian amongst rhyolitic *coulées* (Fig. 5). Specimens of 'geological obsidian were also collected within the caldera. Our analysis of this collection sheds light on lithic procurement on Nabro, enabling us to posit broader implications of a high-elevation, lithic-resource-rich, sporadically-active volcano situated in the prehistoric human orbit of the Eritrean Danakil.

Additionally, the fieldwork furnished the opportunity to observe the extent of 2011 tephra fall deposits and lava flows and their local impacts on vegetation and communities. A substantial population of Afar pastoralists inhabited the area, including more than 3000 people who were resident within the summit caldera of Nabro itself. Several thousand people ended up being permanently relocated (Goitom et al., 2015).

2.2. Argon isotopic measurements

$^{40}Ar/^{39}Ar$ geochronological measurements were performed on a representative suite of trachyte and rhyolite lavas, tephra and ignimbrite samples collected on the flanks of Nabro, the immediately surrounding plains, and within the caldera. In total, 24 samples (one from a rhyolitic pumice fall deposit, eight from rhyolitic or trachytic lava flows, and 15 from ignimbrites) were crushed, sieved and magnetically separated before being immersed in 10% HCl or 15% HF in an ultrasonic bath, followed by ultrasonic rinsing with distilled water to remove the residual acid. The non-magnetic portion was then submerged in heavy liquids to sink quartz and plagioclase feldspar, and float sanidine. Sanidine crystals were handpicked to ensure sample homogeneity using a binocular microscope. All samples and neutron flux monitors were loaded into machined Al discs in a known geometry.

All samples were analysed with a Photon Machines CO_2 laser at the New Mexico Geochronology Research Laboratory connected to a Mass Analyzer Products 215-50 on line mass spectrometer, with an automated all-metal extraction system. Fish Canyon Tuff sanidine (FC-2) was used to monitor the neutron flux (assigned age = 28. 201 Ma; Kuiper et al., 2008). Fish Canyon Tuff sanidine (FC-2) was used to monitor the neutron flux (assigned age = 28. 201 Ma; Kuiper et al., 2008). Single crystals were initially step-heated with the laser to monitor release of gaseous argon. The subsequent analyses were done using single crystal laser fusion to increase signal size and precision. All analytical measurements were collected and reduced using Pychron version 18.2 (Ross, 2014) https://github.com/NMGRL/pychron) and can be found in the Supplemental Material.

2.3. LA-ICP-MS analysis

Laser Ablation Inductively Coupled Plasma Mass Spectrometry (LA-ICP-MS) permits near non-destructive analysis of obsidian artefacts, with laser pits invisible to the naked eye. We analysed ten geological and 24 archaeological obsidian samples collected on and around Nabro at the Centre Ernest-Babelon of the IRAMAT (Orléans) using a Thermofisher Instrument Element XR and a Resonetics Resolution M50E Eximer ArF laser (wavelength of 193 nm). For each selected sample, the concentrations of 38 major, minor and trace elements were determined. These include zirconium, yttrium, niobium, barium, strontium, cerium, lanthanum and titanium, which are particularly effective in classifying distinct geochemical populations amongst obsidian assemblages (e.g., Chataigner and Gratuze, 2014). Specimens were placed in the ablation chamber, where they were sampled by the laser beam. An argon/helium gas flow (1 l min^{-1} Ar and 0.65 l min^{-1} He) carries the ablated aerosol to the injector inlet of the plasma torch, where the matter is dissociated, atomised and ionised. The ions are then injected into the vacuum chamber of a high-resolution system, which discriminates them according to their mass-to-charge ratio. The ions are then collected by a channel electron multiplier or a faraday cup.

The excimer laser operated at energies between 5.5 and 6.5 mJ with a repetition rate of 10 Hz. The beam diameter was adjusted to 100 µm. A pre-ablation time of 20 was is set so as to remove any corrosion layer and the transient part of the signal, and then the sample was measured for 30 s

229 corresponding to 12 mass scans from lithium to uranium (the signal in counts/second was measured
230 in low resolution mode for 38 different isotopes). Only one ablation was carried out for each sample
231 but live counts were monitored during analysis to identify inclusions that could contaminate
232 measurement of the glass composition (Palumbi et al. 2014). Where this was the case, results were
233 discarded and a new ablation site selected. Typical diameter and depth of the ablation crater were
234 100 µm and 150 µm, respectively, but these dimensions varied depending on the ablation duration.

235 The isotope ^{28}Si was used as an internal standard (Chataigner and Gratuze 2014). The standard
236 reference material glasses used for external standardisation were NIST 610 from the National
237 Institute for Standards and Technology and Corning B and D glasses. The standard reference
238 materials glass NIST 612 was repeatedly analysed as an unknown sample to monitor for instrumental
239 drift and to ensure compatibility between different sets of analyses.

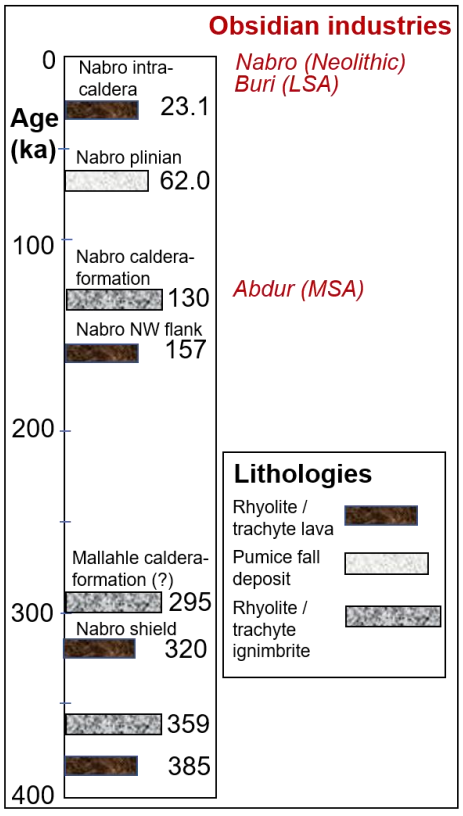

240

241 *Fig. 6. Composite stratigraphy of lavas and pyroclastic deposits dated in this study. See Table 2 for*
242 *detail. Approximate time periods of lithic industries (containing obsidian) in Eritrea as indicated*
243 *(Walter et al., 2000; Beyin, 2011b).*

3. Results and Discussion

3.1. Eruption history

We dated 24 lava and tephra samples by the Ar/Ar method (Table 1; Fig. 6). The oldest specimen is a rhyolitic lava with an age of circa 385 ka, outcropping on the southeast flank of Nabro. This unit lies stratigraphically beneath an unwelded rhyolitic ignimbrite that dates to circa 359 ka. It is unclear if the latter deposit originates from Nabro or Mallahle. Pre-caldera, shield-building rhyolitic and trachytic lavas mantle Nabro's upper flanks and are circa 320 ka old. On the southeast and northwest flanks, and in the southern wall of the caldera are trachytic and rhyolitic ignimbrites that date to circa 295 ka (Fig. 7). Rhyolitic lava flows and coulées, circa 157 ka in age, armour the northwest flanks of Nabro (Fig. 5).

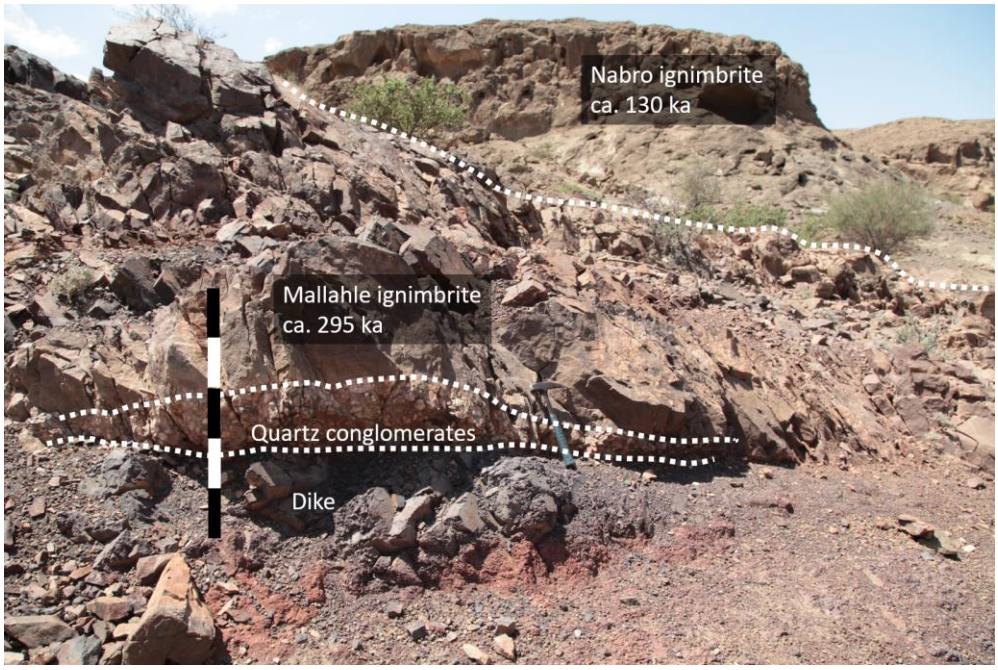

Fig. 7. Stratigraphic relationships observed northwest of Nabro. The circa 295 ka ignimbrite may be sourced from Mallahle though this is uncertain. The conglomerate bed is presumably sourced from the Danakil Alps to the north. Scale bar is 1 m in length.

Unwelded rhyolitic ignimbrites, up to 40-metre-thick where fluvially incised, form a sloping apron that extends to the northwest, north and southeast of Nabro (Fig. 3a). They correspond to the 'eastern' and 'western' ignimbrites (Fig. 1) *sensu* Wiart & Oppenheimer (2005). These date to circa 130 ka, and although there is some scatter between the nine samples, stratigraphic relationships

suggest they belong to the same deposit. We consider that they represent the products of Nabro's last major caldera-forming eruption. Where the deposit remains, it is deeply dissected by *quebrada* reminiscent of Central Andean ignimbrites (Lindsay et al., 2001). Based on the caldera size (Oppenheimer, 2003a), and thickness and radial extent of the ignimbrite (up to 30 km; Wiart & Oppenheimer, 2005), we estimate the magnitude of this eruption to have been comparable to that of the Tambora eruption (Indonesia) of 1815 (Oppenheimer, 2003b).

The youngest pyroclastic rocks that we sampled, which date to circa 62 ka, belong to a tephra fall deposit, remnants of which are found within Nabro's caldera and draping its ramparts and cliffs, and on the volcano's northwest, northeast and southeast flanks (Fig. 1). From its stratigraphic position, thickness and areal extent, it appears to represent the latest major explosive eruption of Nabro. The patchy distribution of the deposit suggests it has been substantially deflated by wind, as seen with the pumice fallout from the 1861 Plinian eruption of neighbouring Dubbi volcano (Wiart & Oppenheimer, 2000). The deposit may be related to pyroclastic density current deposits that outcrop on the southeast flank of Nabro around 11 km from the centre of the caldera. Given the distribution and nature of these pumiceous deposits, we hypothesise that they are associated with the formation of the roughly two-kilometre-diameter crater situated within Nabro's main caldera (that was also the focus of the 2011 eruption). Our youngest sample, at 23.1 ka, is a trachytic lava associated with the eruptive centres within Nabro's main caldera, and close to the vents of the trachybasalt to trachybasaltic andesite eruptions in 2011 (Goitom et al., 2015; Donovan et al., 2018).

3.2. Obsidian tools and source rocks

The suite of obsidian lithics include blades and flakes up to 5–7 cm in length, scrapers, a bladelet core, and a 9-cm-long bipolar core (Table 3). The most recurrent technique observed on characteristic elements is percussion on anvil, but not necessarily with an intention to produce bipolar blanks. The bipolar 'aspect' of the cores appears to be an effect of the anvil technique, rather than of preconceived *débitage* schemes. Retouching is prevalent, often irregular and some evidently significantly younger than the original manufacture, thus suggesting secondary recycling. Our collection also includes small crude flakes, a *pièce esquillée* and a core, a few cm across. Uncollected

surface finds include concentrations of obsidian *débitage* that includes transported blocks of raw material (Fig. 4), indicative of expedient lithic manufacture.

Most formal tool forms that are represented, as well as evidence for elongated blank production (including bladelets and bladelet cores) are typical of the regional Late Pleistocene and Holocene LSA, and were in continued use long after the adoption of ceramic traditions and pastoralism (Hildebrand et al. 2010; Ménard et al. 2014; Leplongeon et al. 2018; Khalidi et al. 2018). The presence of numerous neo-cortical pieces in the assemblage is consistent with the exploitation of local obsidian sources. Obsidian lithics were frequently sighted at the surface while traversing the volcano. In some cases, several pieces were found within a small area (Fig. 4). However, most samples presented here were collected from individual sites. Lacking a systematic survey, we are unable to interrogate spatial or diachronic patterns in tool typology/technology, or source grouping. There is no evidence of prepared core technology or points that might be suggestive of the MSA.

Geochemical analyses of the obsidian samples are reported in Table 2. The compositional range is relatively narrow, spanning approximately 9.5–12.5 wt% Al_2O_3 and 3.3–4.7 wt% FeO_{tot}. These fall mostly within the comenditic field, with a smaller proportion of pantellerites. This geochemical variation can be explained by fractionation of comendite to pantellerite (Scaillet and MacDonald, 2001; 2003). We classify five sub-populations according to trace element distributions (Fig. 8).

The specimens of 'geological' obsidian collected at outcrop fall within three geographical (and two stratigraphic) groupings: rhyolitic lavas on the upper northwest flank (UNWF) and lower northwest flank of Nabro (LNWF; Fig. 5) associated with the circa 157 ka silicic *coulées*; and an intra-caldera source tentatively associated with the 62 ka pumice fall deposit (IC), which may have been formed by sintering of ash within the vent and conduit (e.g., Gardner et al., 2019). These are geochemically distinct as is readily observed in their Sr concentrations: UNWF obsidian has less than 0.3 ppm Sr; LNWF obsidian has Sr concentrations between 1.5 and 1.8 ppm; and IC obsidian has about 4.3–4.9 ppm Sr. Recognising that our sample size is relatively small and that we cannot presume to have characterised the full chemical heterogeneity of the obsidian lavas, we can nevertheless match each

315 of the lithic geochemical clusters with a distinct source. The UNWF obsidian correlates with lithic
316 group 1, the LNWF obsidian with lithic group 3, of which we have just one archaeological sample,
317 while IC obsidian matches lithic group 5 (Fig. 8). Two other geochemically-distinct populations of
318 lithics, groups 2 and 4, are recognised but these may represent sub-populations of the UNWF and
319 LNWF sources, respectively (Fig. 8). It should be borne in mind that while distinct clusters emerge in
320 the element scatter plots, the geochemical variation for the whole collection is small (e.g., all
321 samples have less than 6 ppm Sr, with between 7 and 12 ppm U).

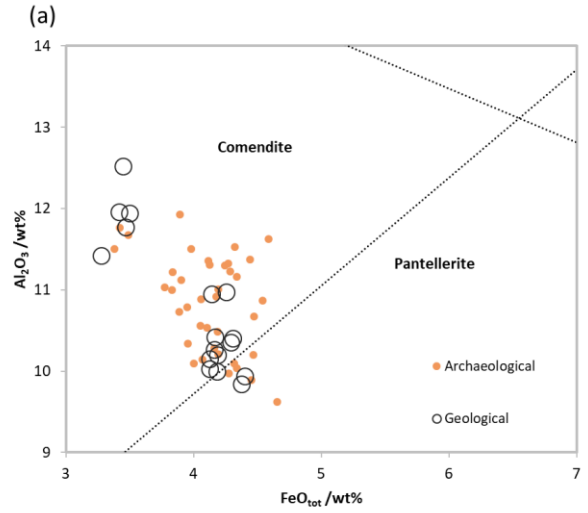

322

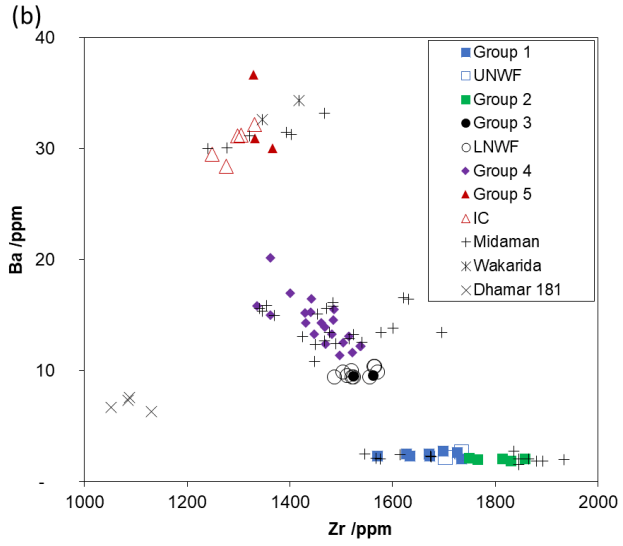

323

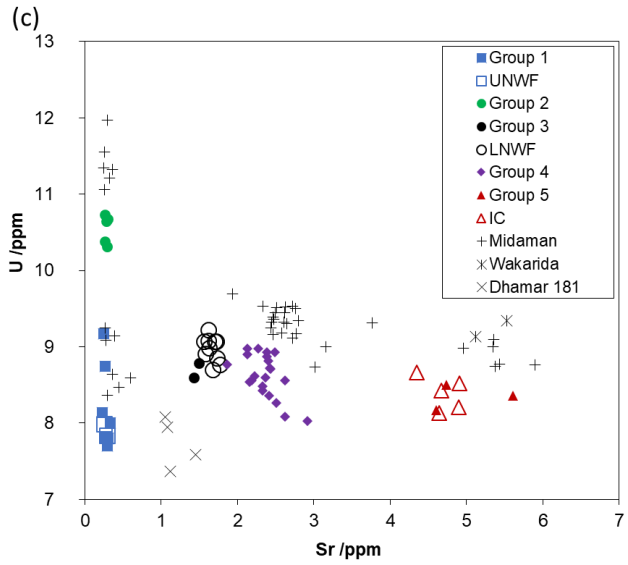

Fig. 8. Geochemical fingerprints of Nabro obsidians (archaeological and geological) along with analyses for artefacts from Yemen (al-Midaman and DS 181) and Ethiopia (Wakarida). Scatter plots for (a) total iron vs. alumina showing petrological classification of Nabro obsidians; (b) zirconium vs. barium; and (c) strontium vs. uranium. Overall, the geochemical variation is quite narrow but three main clusters can be identified: (i) LNWF source and groups 3 and 4 lithics), (ii) UNWF source and groups 1 and 2 lithics), and (iii) IC source and group 5 lithics. See text for elaboration.

Arising from more than a decade of obsidian provenancing in the Southern Red Sea region and adjacent areas, a significant database of obsidian geochemical analyses has been established (e.g., Khalidi et al., 2010; 2013). This permits comparisons to be made with the geochemical signatures of our Nabro samples (Table 4; Fig. 8). We find matches between Nabro obsidian and a total of 37 lithics from two archaeological sites, one in Ethiopia and the other across the Red Sea in Yemen. The first correspondence is with the Aksumite site of Wakarida (3rd to 8th c. CE), over 200 km distant in the Tigray region at the crest of the Ethiopian plateau (Gajda et al., 2015). Here, a single artefact matches the IC source and group 5 Nabro lithics. For the Bronze Age site of al-Midaman (3rd to 2nd millennium BCE) in the Tihamah (Yemen; Keall, 1998; 2005; Khalidi et al. 2018), linear distance of around 190 km from Nabro, we find matches for 36 artefacts. The majority correlates with group 4 Nabro lithics, i.e., close to the signature of the LNWF source but there are further clusters of al-

Midaman lithics that correspond with groups 1 and 2 (UNWF) and 5 (IC), amongst the Nabro obsidian collection.

Two artefacts from the Himyarite and Late Islamic period site of Dhawran, DS 181, in the Dhamar region of the Yemen highland plateau (Wilkinson & Edens, 1999), more than 300 km away, are closer to the Nabro material geochemically than any other obsidian, but the correspondence cannot be confirmed with the available source material. Dhawran was the late Islamic capital of Yemen during the time of the Qasimi imam al Mutawakkil (reigned 1644-1676 CE; see Wilkinson & Edens, 1999; Dresch 1989: 200).

3.3 Socio-cultural perspectives

Amongst our obsidian artefact assemblage, there is clear evidence of lithic traditions associated with potter-pastoralists elsewhere in Afar (Neolithic: Diaz, 2016; Gutherz et al., 2015; Cauliez et al., 2017; Khalidi et al., 2018) and on the Red Sea coast of Yemen (Bronze Age: Buffa & Vogt 2001; Khalidi, 2005; Crassard, 2008). The suite of samples testifies to the exploitation of a high-quality (homogeneously glassy) obsidian resource exposed on the landscape for tens of thousands of years. The local production of tools and the high terrain of the caldera floor and associated cool and wet environment compared with the surrounding desert lowlands suggest to us that Nabro may have been settled and/or frequented in the Late Pleistocene and Holocene by pastoralists and hunter-gatherers. A systematic survey might reveal quarries and tool manufacture sites, especially on the high-quality obsidian outcrops associated with the LNWF and UNWF flows. Future work can also be expected to yield clearer insights into the antiquity and continuity or episodes of prehistoric and historical exploitation and occupation of Nabro.

All three primary sources of obsidian found on Nabro are represented in lithic assemblages both on and in the vicinity of the volcano, and at distal sites: on the crest of the Ethiopian plateau at Wakarida, at the coastal Tihamah site of al-Midaman, and possibly on the Yemen plateau at the Dhamar Survey Project site 181. These sites at different azimuths and ranges from Nabro, and at considerable range, point to shifting networks of interaction between the coastal lowlands and highlands on both sides of the Red Sea over timescales of millennia. That Nabro obsidian was so

widely exchanged and represents such a significant proportion of obsidian lithics at the al-Midaman site suggests that the raw material available on Nabro, especially that of the lavas on the northwest flank of the volcano, was well known and held in high regard.

Nabro and Mallahle are so close to each other that we can expect their deposits to be, in places, interleaved. Furthermore, given the limited scope for reconnaissance in the field (and without access to the Ethiopian side of the international border), we cannot fully disambiguate the origin of the tephra deposits we encountered. Nevertheless, we have identified evidence for several large eruptions of Nabro and Mallahle volcanoes (circa 359, 295, 157 and 62 ka ago), testifying to their transformations and looming presence in the Southern Red Sea landscape since the Middle Pleistocene. Rhyolitic lavas that yielded a source of high-quality obsidian were erupted around 157 ka ago on Nabro's northwest slopes. We cannot yet say when these were first exploited, but any local traces and signs of human activity within approximately 30 km of the volcano would likely have been obliterated at the time of the volcano's last caldera-forming eruption circa 130 ka ago. The associated pyroclastic deposits would also have buried the 157 ka rhyolitic lava flows and associated LNWF obsidian source (from which the group 2 artefacts were manufactured). Considering the evidence for human occupation along the Gulf of Zula coastline (less than 300 km distant) dated to circa 125 ka ago (Walter et al., 2000), and the geographical extent of volcanic ash clouds and ash fallout associated with very large eruptions, we conjecture that the 130 ka eruption was experienced by contemporary human populations. Any MSA exploitation of the LNWF obsidian that may have occurred prior to the caldera-forming eruption would have been disrupted until erosion of the tephra re-exposed the older lavas. While we have not dated the UNWF lavas, stratigraphic relationships suggest they also pre-date the caldera.

A younger obsidian source, tentatively dated to around 62 ka, was used by prehistoric pastoralists on either side of the Red Sea. We speculate that a more systematic survey of the terrain would yield evidence for obsidian exploitation in the MSA, which is represented in obsidian assemblages from the Buri peninsula (Beyin and Shea, 2007), approximately 300 km northwest, a range of transport that was achieved elsewhere in the MSA of eastern Africa (Negash et al., 2011; Blegen, 2018).

The timing of the caldera-forming eruption of Nabro assumes further significance in the context of emerging evidence for temporal clustering of major eruptions in the Main Ethiopian Rift in the Middle Pleistocene (Hutchison et al., 2016). The volcanic events at circa 130 and 62 ka may be represented in regional sedimentary archives as distal tephra deposits in terrestrial, lacustrine and marine (Red Sea, Gulf of Aden, Lake Tana) contexts, and conceivably as aerosol markers in polar ice cores. Tephrastratigraphic correlations might thereby provide valuable chronological orientation for archaeological materials or paleoenvironmental archives.

The Danakil region is generally dry, extremely hot, and sparsely populated. Its present-day inhabitants are mostly pastoralists keeping herds of sheep, goats, camels, donkeys and cattle. Nabro's elevation is associated with a cooler and wetter microclimate compared with the desert plains (the caldera floor lies at about 1400 m above sea level), making it conducive to settlement. Sireru, a community that was located in the southern part of the caldera before the 2011 eruption had a human population of around 3000. Run-off was harvested and stored in lined ponds shaded from evaporative losses by brush canopies. Steam vents within the caldera were used therapeutically and may have provided additional fresh water through use of artisanal condensation systems, as seen elsewhere in the Danakil (e.g., Nebro et al., 2016).

The humanitarian crisis following the 2011 eruption was exacerbated by the proximity of Sireru and two other villages – Mindig and Maebele – to the active vents and fissures. Sireru remains buried by tephra and abandoned – a 'Pompeii' of Afar (Fig. 9). Around 12,000 former inhabitants of the caldera and flanks of the volcano were displaced and relocated in Wade (Goitom et al., 2015), 30 km to the southeast, Hawra, 30 km north, and Alaile, near the city of Assab, around 100 km to the southeast. Those who were relocated to Wade and Hawra continued pastoralism, while the inhabitants of Alaile had to adopt new livelihoods such as fishing and trading. Many could not adapt and returned to the southern slopes of Nabro. While Sireru remains uninhabitable, the nearby slopes are used for grazing. We learned that one group of the returnees had started to reuse a cavern in the caldera wall to keep their goats in at night, as they had done before the eruption. On 25 April 2016, following a

day of heavy rainfall in the area, 253 of the goats were found dead, possibly due to volcanic CO_2 poisoning.

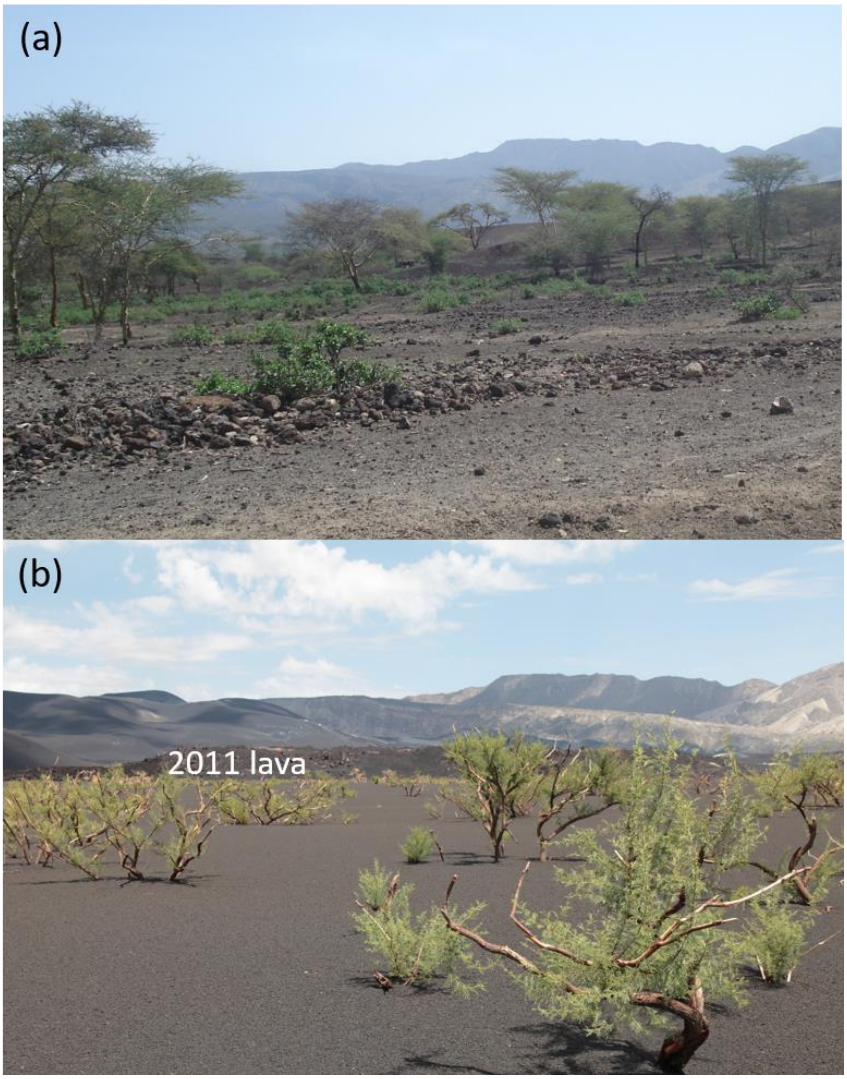

Fig. 9. Burial of Sireru settlement and vegetation by 2011 tephra fall deposits: (a) pre-eruption, (b) post-eruption (compare the caldera outlines to situate the two photographs in relation to each other). Remarkably, acacia trees survive despite near total burial in scoria deposits (up to several metres in thickness) and abrasion of bark by falling scoriae. In the middle ground in (b) note also the front of a lava flow that issued from the 2011 vent region. This illustrates how eruption deposits can modify hydrology, impact vegetation, and bury occupation surfaces (and obsidian resources).

This contemporary experience of settlement, abandonment and re-occupation highlights the risks and rewards of living close to a dormant volcano and may, in some sense, represent an echo of past human experiences on the volcano. The 2011 eruption may also offer a rare opportunity to

document the ecological succession in landscapes of varying elevation that were inundated by lava flows and/or covered in tephra fallout and subject to hyper-arid climate. While the 2011 eruption was diminutive in comparison with the caldera-forming events that shaped Nabro and Mahllale, as well as other volcanoes in Afar and the Rift, it may yet furnish valuable insights into the nature and extent of ecological and hydrological impacts of colossal eruptions of the region in the past.

4. Conclusions

Individual volcanoes that dominate the landscape today have lifespans that can exceed human evolutionary timescales, yet when they awaken, their impacts are immediate and transformative on the scale of human lifetimes. Such volcanoes are mutable: their stratigraphies may be palimpsests of both volcanic and human traces. We have traced key stages in the life history of Nabro volcano (and its immediate neighbour Mallahle), charting transitions from devastation to opportunity for human populations. We cannot say yet when people first took advantage of the opportunities of high calderas and their lithic resource but the evidence for MSA and LSA occupation of the Red Sea littoral of Eritrea, and the quality and comparative scarcity of obsidian sources in the predominantly basaltic terrain lead us to speculate that it likely stretches back through the Upper Pleistocene. At the least, aspects of the regional late prehistoric economy were anchored on Nabro.

While our resumé of Nabro's stratigraphy can only capture parts of the eruptive history of the volcano, at least two major explosive eruptions occurred, circa 130 and 62 ka ago, during the time that modern humans occupied the Danakil. These events would have disrupted access to obsidian resources (including the products of effusive eruptions circa 157 ka ago), though, on the other hand, the circa 62 ka eruption yielded a new obsidian source. More detailed fieldwork in the region might identify sedimentary sequences bracketed by the major eruptive episodes, offering the prospect of new archaeological discoveries.

In the Danakil desert today, elevated caldera floors receive sufficient rainfall to support farming and pastoralism. These volcanoes dominate the plains that stretch to the Red Sea and have likely represented sacred places or supernatural realms (e.g., Erta 'Ale in Ethiopia; Oppenheimer and Francis, 1997) as well as visual anchors (see, for example, Bernadini *et al*., 2013). The wide

distribution of obsidian tools indicates that they may also have acted as habitable, resource-rich hubs connected to the coast. Such connections would have endured throughout the significant sea-level and climate-driven landscape changes of the Late Pleistocene but would have been interrupted by large and unpredictable volcanic events.

The extent and thickness of tephra fallout from Nabro's 2011 eruption was comparatively modest compared with that evident from prior eruptions. Nevertheless, settled areas were partly or completely buried; some settlements and kraals were engulfed by lava flows. This episode provides insights into the interplay of long-term opportunity (lithic resource, microclimate, strategic location) afforded by high calderas, and the sporadic but major dislocations and landscape transformations accompanying large eruptions. Volcanic devastation can reshape and rejuvenate cultural landscapes – both in terms of the formation of wide calderas, and in the production of new lithic resources. The diversity, dynamism and accessibility of connected highland caldera and coastal landscapes in the Danakil desert would have offered both opportunities and sanctuaries throughout prehistory.

Between Eritrea, Ethiopia and Kenya, there are more than two dozen silicic caldera volcanoes of likely Quaternary age. In addition to Mallahle and Nabro, also of note are Ma'alalta, Fentale, Kone, Gedemsa, Aluto, Shala and Corbetti in Ethiopia, and Suswa and Menengai in Kenya. Caldera diameters range from 5 to 17 km and several of the volcanoes are associated with presently active magmatic systems (Biggs et al., 2009) and prized obsidian sources (Goldstein et al., 2017; Blegen et al., 2017). Large calderas, some known to host obsidian sources, are also to be found in the Tibesti of northern Chad. The eruptive and erosive histories of many of these volcanoes span all or part of the history of our genus – we argue that their significance for understanding aspects of human behaviour and culture in deep antiquity goes far beyond tephrochronological dating and merits deeper investigation.

The 2011 eruption also draws attention to the limitations in Eritrea's present capacity for study and characterisation of geohazards (e.g., Goitom et al., 2017). The 2011 eruption of Nabro claimed seven lives and displaced many thousands (Goitom et al., 2015); the 1861 eruption of neighbouring Dubbi

volcano reportedly claimed as many as 175 lives (Wiart and Oppenheimer, 2000). We hope this paper may help to stimulate more detailed and systematic investigation of eruption and habitation histories in Eritrea. This can contribute not only to understanding the region's deep history but can also inform management of contemporary disaster risk in the region.

Acknowledgements

This work was supported by the UK Natural Environment Research Council (project # NE/J012297/1 "Mechanisms and implications of the 2011 eruption of Nabro volcano, Eritrea"), and Leverhulme Trust ("Nature and impacts of Middle Pleistocene volcanism in the Ethiopian Rift"). We thank Iwona Gajda, who along with Anne Benoist directed the French-Ethiopian collaborative project, *Recherches archéologiques et épigraphiques dans la région duTigray, Éthiopie*, for providing the obsidian samples from Wakarida, and the Royal Ontario Museum for loan of the material from al-Midaman. We are grateful to Goitom Kibrom for assistance with the fieldwork in Eritrea; and Alex Wilshaw, Bruno Scaillet, Rob Foley and Marta Lahr for discussions.

References

Al-Abri, A., E. et al. (2012). Pleistocene-Holocene Boundary in Southern Arabia: From the Perspective of Human mtDNA Variation. *American Journal of Physical Anthropology* 2012: 1-8.

Ambrose, S. H. (2012). Obsidian Dating and Source Exploitation Studies in Africa. In Liritzis, I. and Stevenson, C.M., *Obsidian and Ancient Manufactured Glasses*. University of New Mexico Press, 240pp.

Armitage, S. J., et al. (2011). The southern route "out of Africa": Evidence for an early expansion of modern humans into Arabia. *Science*, *331*, 453-456

Bailey, G. N. & King, G. C. P. 2011, Dynamic landscapes and human dispersal patterns: Tectonics, coastlines, and the reconstruction of human habitats. *Quat. Sci. Rev*. 30**,** 1533–1553.

Bailey, G., et al. (2008). The coastal shelf of the Mediterranean and beyond: Corridor and refugium for human populations in the Pleistocene. *Quaternary Science Reviews* 27: 2095-2099

512 Barberi, F., Tazieff, H. and Varet, J., 1972. Volcanism in the Afar depression: its tectonic and
513 magmatic significance. *Tectonophysics*, *15*,19-29.

514 Basell, L.S., 2008. Middle Stone Age (MSA) site distributions in eastern Africa and their relationship
515 to Quaternary environmental change, refugia and the evolution of Homo sapiens. *Quaternary*
516 *Science Reviews*, *27*, 2484-2498.

517 Bernadini, W., Barnash, A., Kumler, M., and Wong, M., 2013, Quantifying visual prominence in social
518 landscapes, Journal of Archaeological Science, 40, 3946-3954.

519 Beyin, A. (2011a). Upper Pleistocene Human Dispersals out of Africa: A Review of the Current State
520 of the Debate. *International Journal of Evolutionary Biology* 2011: 1-17

521 Beyin, A. (2011b). Early to Middle Holocene human adaptations on the Buri Peninsula and Gulf of
522 Zula, coastal lowlands of Eritrea. *Azania: Archaeological Research in Africa*, *46*(2), 123-140.

523 Beyin, A. and Shea, J.J., 2007. Reconnaissance of prehistoric sites on the Red Sea coast of Eritrea, NE
524 Africa. *Journal of Field Archaeology*, *32*(1), 1-16.

525 Biggs, J., Anthony, E.Y. & Ebinger, C.J., 2009, Multiple inflation and deflation events at Kenyan
526 volcanoes, East African Rift, *Geology*, 37, 979–982.

527 Blegen, N., 2017. The earliest long-distance obsidian transport: Evidence from the ~ 200 ka Middle
528 Stone Age Sibilo School Road Site, Baringo, Kenya. *Journal of human evolution*, *103*, pp.1-19.

529 Buffa, V. and Vogt, B. 2001 Sabir - Cultural Identity between Saba and Africa. In Migration und
530 Kulturtransfer. Der Wandel vorder- und zentralasiatischer Kulturen im Umbruch vom 2. Zum 1.
531 Vorchristlichen Jahrtausend, Kolloquien zur Vor- und Fruhgeschichte 6 (Akten des Internationalen
532 Kolloquiums, Berlin November 1999), Habelt, Bonn., edited by R. Eichmann and H. Parzinger, pp.
533 437-450. vol. 2:1. Dr. Rudolf Habelt GmbH, Bonn, Berlin.

534 Cauliez, J., Gutherz, X. and Pène, J.-M. 2017 Asa Koma et les traditions céramiques néolithiques
535 de la région du Gobaad. In *Asa Koma : Site néolithique dans le bassin du Gobaad (République de*
536 *Djibouti)*, edited by X. Gutherz, pp. 67-142.

537 Chataigner, C. and Gratuze, B., 2014. New Data on the Exploitation of Obsidian in the S outhern C
538 aucasus (A rmenia, G eorgia) and Eastern T urkey, Part 1: Source Characterization. *Archaeometry*,
539 *56*(1), 25-47.

540 Coudert, L., Lesur, J., Bruxelles, L., Gutherz, X. and Cauliez, J., 2018. New archaeozoological results
541 from Asa Koma (Djibouti): Contributing to the understanding of faunal exploitation during the 3rd
542 millennium BC in the Horn of Africa. *Quaternary International*, *471*, pp.219-228.

543 Crassard, R. 2008 La préhistoire du Yémen: Diffusions et diversités locales, à travers l'étude
544 d'industries lithiques du Hadramawt BAR S1842. Archaeopress, Oxford.

545 Dale, V.H., Swanson, F.J. and Crisafulli, C.M., 2005. *Ecological responses to the 1980 eruption of*
546 *Mount St. Helens*(p. 342). New York: Springer.

547 del Moral, R. and Magnússon, B.: Surtsey and Mount St. Helens: a comparison of early succession
548 rates, Biogeosciences, 11, 2099-2111, https://doi.org/10.5194/bg-11-2099-2014, 2014.

549 Diaz, A. 2016. Les industries lithiques des sites d'habitat des premiers éleveurs du bassin du Gobaad
550 en République de Djibouti : apport de la technologie lithique à la caractérisation des cultures des
551 premières sociétés de production. PhD. Histoire, Université Paul Valéry - Montpellier III.

552 Donovan, A, Blundy J, Oppenheimer C, Buisman I (2018) The 2011 eruption of Nabro volcano,
553 Eritrea: perspectives on magmatic processes from melt inclusions. *Contrib Mineral Petrol* 173(1):1.

554 Dresch, P. 1989 *Tribes, Government and History in Yemen*. Clarendon Press, Oxford.

555 Dumitru, I.A. and Harrower, M., 2018. Mapping Ancient Production and Trade of Copper in Oman
556 and Obsidian in Ethiopia. In *Stories of Globalisation: The Red Sea and the Persian Gulf from Late*
557 *Prehistory to Early Modernity* (pp. 74-94). BRILL.

Gajda, I., Benoist, A., Charbonnier, J., Antonini, S., Peixoto, X., Verdellet, C., Bernard, V., Barge, O., Regagnon, E. and Callot, Y., 2015. Wakarida, un site aksumite à l'est du Tigray: fouilles et prospections 2011-2014/Wakarida, an Aksumite Site in Eastern Tigray: Excavations and Surveys 2011-2014. In *Annales d'Éthiopie* (Vol. 30, No. 30, pp. 177-224).

Gardner, J.E., Wadsworth, F.B., Llewellin, E.W., Watkins, J.M. and Coumans, J.P., 2019. Experimental constraints on the textures and origin of obsidian pyroclasts. *Bulletin of Volcanology*, *81*, 22.

Ge, C., J. Wang, S. Carn, K. Yang, P. Ginoux, and N. Krotkov (2016), Satellite-based global volcanic SO_2 emissions and sulfate direct radiative forcing during 2005–2012, *J. Geophys. Res. Atmos.*, 121, 3446–3464, doi:10.1002/2015JD023134.

Goitom, B., Oppenheimer, C., Hammond, J.O., Grandin, R., Barnie, T., Donovan, A., Ogubazghi, G., Yohannes, E., Kibrom, G., Kendall, J.M. and Carn, S.A., 2015. First recorded eruption of Nabro volcano, Eritrea, 2011. *Bulletin of Volcanology*, doi: 10.1007/s00445-015-0966-

Goitom, B., Werner, M.J., Goda, K., Kendall, J.M., Hammond, J.O., Ogubazghi, G., Oppenheimer, C., Helmstetter, A., Keir, D. and Illsley-Kemp, F., 2017. Probabilistic seismic-hazard assessment for Eritrea. *Bulletin of the Seismological Society of America*, *107*, 1478-1494.

Goldstein, S.T. and Munyiri, J.M., 2017. The Elmenteitan Obsidian Quarry (GsJj50): new perspectives on obsidian access and exchange during the Pastoral Neolithic in southern Kenya. *African Archaeological Review*, *34*(1), pp.43-73.

Gutherz, X., Lesur, J., Cauliez, J., Charpentier, V., Diaz, A., Ismaël, M. O., Pène, J.-M., Sordoillet, D. and Zazzo, A. 2015, New insights on the first Neolithic societies in the Horn of Africa: The site of Wakrita, Djibouti. *Journal of Field Archaeology* 40(1):55-68.

Hamlyn, J., Wright, T., Walters, R., Pagli, C., Sansosti, E., Casu, F., Pepe, S., Edmonds, M., Kilbride, B.M., Keir, D., Neuberg, J. and Oppenheimer, C., 2018. What causes subsidence following the 2011 eruption at Nabro (Eritrea)?. *Progress in Earth and Planetary Science*, *5*(1), p.31.

582 Hammond, H., Goitom, B., Kendall, M., Ogubazghi, G., Oppenheimer C. (2011): Nabro Urgency Array.
583 International Federation of Digital Seismograph Networks. Other/Seismic Network.
584 10.7914/SN/4H_2011

585 Hildebrand, E. A., Brandt, S. A. and Lesur-Gebremariam, J. 2010 The Holocene Archaeology of
586 Southwest Ethiopia: New Insights from the Kafa Archaeological Project. *African Archaeological*
587 *Review* 27(4):255-289.

588 Hutchison et al., 2016, A pulse of mid-Pleistocene rift volcanism in Ethiopia at the dawn of modern
589 humans. *Nature Communications*, doi:10.1038/ncomms13192

590 Institut San'a'. vol. Band X. Verlag Phillip Von Zabern, Mainz am Rhein.

591 Keall, E. J. 2005 Placing al-Midamman in time. The work of the Canadian Archaeological Mission on
592 the Tihama coast, from the Neolithic to the Bronze Age. In *Archäologische Berichte aus dem Yemen*,
593 pp. 87-99. Deutsches Archäologisches

594 Keall, E.J., 1998, January. Encountering megaliths on the Tihāmah coastal plain of Yemen. In
595 *Proceedings of the Seminar for Arabian Studies* (Vol. 28, pp. 139-147). Archaeopress.

596 Khalidi, L. (2009). Holocene Obsidian Exchange in the Red Sea Region. In *The Evolution of Human*
597 *Populations in Arabia: Paleoenvironments, Prehistory and Genetics* edited by M. D. Petraglia and J. I.
598 Rose, pp. 279-291. Vertebrate Paleobiology and Paleoanthropology. Dordrecht: Springer

599 Khalidi, L. 2005 The Prehistoric and Early Historic Settlement Patterns on the Tihamah Coastal Plain
600 (Yemen): Preliminary Findings of the Tihamah Coastal Survey 2003. *Proceedings of the Seminar for*
601 *Arabian Studies* 35:115-127.

602 Khalidi, L., Cauliez, J., Bon, F., Bruxelles, L., Gratuze, B., Lesur, J., Menard, C., Gutherz, X., Crassard, R.
603 and Keall, E. 2018 Late prehistoric oasitic niches along the southern Red Sea (Yemen and Horn
604 of Africa). In *From refugia to oases: Living in arid environments from prehistoric times to the present*
605 *day, XXXVIIIe rencontres internationales d'archéologie et d'histoire d'Antibes*, edited by L. Purdue, J.
606 Charbonnier and L. Khalidi, pp. 71-99. Éditions APDCA, Antibes.

Khalidi, L., Oppenheimer, C., Gratuze, B., Boucetta, S., Sanabani, A. and Al-Mosabi, A., 2010. Obsidian sources in highland Yemen and their relevance to archaeological research in the Red Sea region. *Journal of Archaeological Science*, *37*(9), pp.2332-2345.

King, G. & Bailey, G., 2006, Tectonics and human evolution, *Antiquity*, 80, 265–286.

Kingston, J. D. (2007). Shifting adaptive landscapes: progress and challenges in reconstructing early hominid environments. *American Journal of Physical Anthropology*, *134*(S45), 20-58.

Kuiper, K. F., Deino, A., Hilgen, F. J., Krijgsman, W., Renne, P. R., Wijbrans, J. R. (2008). Synchronizing Rock Clocks of Earth History. *Science 320, 500-504, doi: 10.1126/science.*

Lahr, M. M., & Foley, R. (1994). Multiple dispersals and modern human origins. Evolutionary Anthropology: Issues, News, and Reviews, 3(2), 48-60

Leplongeon A, Pleurdeau D, Hovers E. 2017. Late Pleistocene and Holocene Lithic Variability at Goda Buticha (Southeastern Ethiopia): Implications for the Understanding of the Middle and Late Stone Age of the Horn of Africa. *J. Afr. Archaeol.* 15: 1-32.

Lesur, J. 2014, Emergence du pastoralisme dans la Corne de l'Afrique : adaptations culturelles et environnementales en contexte tropical. *Bulletin des Séances. Académie Royale des Sciences d'Outre-Mer* 60(2014-2):299-317.

Lesur-Gebremariam, J. (2009). Origine et diffusion de l'élevage dans la Corne de l'Afrique: Un état de la question. *Annales d'Éthiopie* XXIV: 173-208

Lindsay, J. M., De Silva, S., Trumbull, R., Emmermann, R., & Wemmer, K. (2001). La Pacana caldera, N. Chile: a re-evaluation of the stratigraphy and volcanology of one of the world's largest resurgent calderas. *Journal of Volcanology and Geothermal Research*, *106*, 145-173

Maslin, M. et al. 2014, East african climate pulses and early human evolution. Quat. Sci. Rev. 101, 1–17.

Ménard, C., et al. (2014). Late Stone Age variability in the Main Ethiopian Rift: New data from the Bulbula River, Ziway–Shala basin. *Quaternary International*, *343*, 53-68.

Morgan, L.E., Renne, P.R., Taylor, R.E. and WoldeGabriel, G., 2009. Archaeological age constraints from extrusion ages of obsidian: Examples from the Middle Awash, Ethiopia. *Quaternary Geochronology*, *4*(3), pp.193-203.

Munro-Hay, S. C. H. (1982). The Foreign Trade of the Aksumite Port of Adulis. *Azania* 17: 107-125

Nebro, A., Gardo, I.A., Varet, J. and Onyango, S., 2016. Community-based geothermal development perspective in Afar: a new player Afar Geothermal Development Company (AGAPI). In *Proceedings, 6th African Rift Geothermal Conference, Addis Ababa, Ethiopia*.

Negash A, Brown F, Nash B. 2011. Varieties and sources of artifactual obsidian in the Middle Stone Age of the Middle Awash, Ethiopia. *Archaeometry* 53(4): 661-673.

Oppenheimer, C., 2003a, Ice core and palaeoclimatic evidence for the timing and nature of the great mid-13th century volcanic eruption, *International Journal of Climatology*, 23, 417–426.

Oppenheimer, C., 2003b, Climatic, environmental and human consequences of the largest known historic eruption: Tambora volcano (Indonesia) 1815, *Progress in Physical Geography*, 27, 230–259.

Oppenheimer, C., 2011, *Eruptions that shook the world*, Cambridge University Press, 408 pp.

Oppenheimer, C., and Francis, P., 1997, Remote sensing of heat, lava and fumarole emissions from Erta 'Ale volcano, Ethiopia, *International Journal of Remote Sensing*, 18, 1661-1692.

Oppenheimer, S. (2012). A single southern exit of modern humans from Africa: Before or after Toba? Quaternary International, 258, 88–99.

Oppenheimer, S., 2009, The great arc of dispersal of modern humans: Africa to Australia, *Quaternary International*, 202, 2–13.

652 Palumbi, G., Gratuze, B., Harutyunyan, A. and Chataigner, C., 2014. Obsidian-tempered pottery in
653 the Southern Caucasus: a new approach to obsidian as a ceramic-temper. *Journal of Archaeological*
654 *Science*, *44*, 43-54.

655 Raunig, W. (2004). Adulis to Aksum: charting the course of antiquity's most important trade route in
656 East Africa. In *Trade and Travel in the Red Sea Region*, edited by P. Lunde and A. Porter, pp. 87-91.
657 Society for Arabian Studies Monographs No.2 and BAR International Series 1269, Archaeopress,
658 Oxford

659 Rose, J. I., V. Cern_y and R. Bayoumi. (2013). Tabula rasa or refugia? Using genetic data to assess the
660 peopling of Arabia. *Arabian archaeology and epigraphy* 24: 95-101

661 Ross, J.R. 2014. Geochronology of Southern McMurdo Sound and development of Pychron: A
662 $^{40}Ar/^{39}Ar$ data collection and processing software suite. PhD Dissertation, Department of Earth and
663 Environmental Science New Mexico Institute of Mining and Technology, USA; Socorro, NM, 87801

664 Sahle Y, Beyin A. 2017. Archaeological reconnaissance of the Late Pleistocene Red Sea coast in the
665 Danakil. *Antiquity* 91(395), e2: 1-6.

666 Scaillet, B. and Macdonald, R., 2001. Phase relations of peralkaline silicic magmas and petrogenetic
667 implications. *Journal of Petrology*, *42*(4), pp.825-845.

668 Scaillet, B. and Macdonald, R., 2003. Experimental constraints on the relationships between
669 peralkaline rhyolites of the Kenya Rift Valley. *Journal of Petrology*, *44*(10), pp.1867-1894.

670 Trauth, M. H., et al., (2010). Human evolution in a variable environment: the amplifier lakes of
671 Eastern Africa. *Quaternary Science Reviews*, *29*(23), 2981-2988.

672 Walter *et al*. (2000). Early human occupation of the Red Sea coast of Eritrea during the last
673 interglacial, *Nature*, 405, 65–69

674 Whittaker, R.J., Bush, M.B. and Richards, K., 1989. Plant recolonization and vegetation succession on
675 the Krakatau Islands, Indonesia. *Ecological Monographs*, *59*(2), pp.59-123.

676 Wiart, P. & Oppenheimer, C., 2005, Large magnitude silicic volcanism in north Afar: The Nabro
677 Volcanic Range and Ma'alalta volcano, *Bulletin of Volcanology*, 67, 99-115

678 Wiart, P. and Oppenheimer, C., 2000. Largest known historical eruption in Africa: Dubbi volcano,
679 Eritrea, 1861. *Geology*, *28*(4), 291-294.

680 Wilkinson, T. J. and Edens, C. (1999), Survey and Excavation in the Central Highlands of Yemen:
681 Results of the Dhamār Survey Project, 1996 and 1998. Arabian Archaeology and Epigraphy, 10: 1-33.
682 doi:10.1111/j.1600-0471.1999.tb00124.x

683

684 Table 1. Summary of single crystal (sanidine) Ar/Ar measurements. All errors are reported at ±2σ,
685 unless otherwise noted.

Sample	**Lithology**	***n***	**MWSD**	**K/Ca**	**Age (ka) ± 2σ**
		Nabro intracaldera eruption			
NAB-11-55	Rhyolite lava	20/20	1.52	3.50	23.1 ± 3.8
		Nabri plinian eruption			
NAB-11-22	Rhyolite tephra fallout	5/8	2.18	8.01	62.0 ± 9.1
		Nabro caldera formation			
NAB-11-46	Ignimbrite	12/27	2.48	N/A	125.3 ± 2.0
NAB-11-41	Ignimbrite	10/27	0.36	60.93	127.7 ± 0.8
NAB-11-36	Ignimbrite	12/35	1.68	82.09	129.4 ± 1.4
NAB-11-34	Ignimbrite	6/27	0.44	27.90	129.7 ± 1.2
NAB-11-103	Ignimbrite	7/34	2.00	150.14	129.8 ± 1.4
NAB-11-42	Ignimbrite	14/29	2.05	25.90	130.0 ± 1.6
NAB-11-1	Ignimbrite	5/23	0.82	162.77	131.7 ± 1.0
NAB-11-104	Ignimbrite	12/33	0.42	18.97	132.5 ± 1.3
NAB-11-35	Ignimbrite	9/24	2.88	14.66	133.9 ± 2.0
		Rhyolite lava flows & coulees on northwest flank of Nabro			
NAB-11-26	Rhyolite lava	4/8	0.58	217.01	156.4 ± 2.4
NAB-11-17	Rhyolite lava	3/7	11.73	1293.80	158.6 ± 4.1
		Mallahle (?) caldera formation			
NAB-11-93	Rhyolitic ignimbrite	8/10	0.13	47.62	293.4 ± 0.8
NAB-11-39	Trachytic ignimbrite	9/10	3.00	65.32	294.8 ± 1.4
NAB-11-90	Trachyte lava	10/10	1.27	37.60	294.9 ± 1.3

NAB-11-40	Trachytic ignimbrite	11/14	0.49	37.76	295.1 ± 1.1
NAB-11-82	Trachytic ignimbrite	10/10	2.70	24.79	295.6 ± 2.0
NAB-11-9	Trachyte lava	3/8	0.21	18.18	300.3 ± 6.6
		Nabro shield construction			
NAB-11-69	Rhyolite lava	8/10	1.26	15.40	318.8 ± 3.5
NAB-11-50	Trachyte lava	7/10	0.57	34.10	323.2 ± 1.4
		Earlier episodes			
NAB-11-92	Rhyolitic ignimbrite	6/10	1.28	63.57	358.8 ± 1.5
NAB-11-91	Rhyolitic ignimbrite	20/20	1.77	7.88	358.9 ± 4.6
NAB-11-72	Rhyolite lava	9/9	3.22	3.14	384.9 ± 9.6

686

687

Table 2. Average compositions (and standard deviations) of Nabro geological and archaeological obsidian samples. Elements with contents above 0.1 % are expressed in weight % of oxides, other elements are given in parts per millions of elements. Some samples were analysed multiple times to verify homogeneity. Numbers of different samples and numbers of analysis carried out are reported as follows: av. (number of samples/number of analyses).

Group		**Na_2O**	**Al_2O_3**	**SiO_2**	**K_2O**	**CaO**	**TiO_2**	**MnO**	**Fe_2O_3**	**ZrO_2**	**Li**	**B**	**Mg**	**Sc**	**Zn**	**Rb**	**Sr**	**Y**	**Nb**	**Cs**
UNWF (geological)	av. (1/3)	5.28	11.0	73.6	4.37	0.43	0.255	0.122	4.51	0.232	38.9	12.0	20.0	12.8	264	176	0.29	110	266	1.68
1	std.	0.08	0.12	0.3	0.05	0.03	0.012	0.005	0.09	0.002	0.4	0.4	1.1	1.6	21	3	0.04	2	10	0.07
Group 1 (UNWF)	av. (6/8)	5.28	10.9	73.5	4.38	0.45	0.259	0.122	4.63	0.225	39.5	12.3	21.0	14.8	272	184	0.28	112	269	1.76
6	std.	0.18	0.7	1.0	0.18	0.08	0.007	0.004	0.22	0.007	1.2	0.8	1.2	2.4	34	9	0.03	6	8	0.14
Group 2 (UNWF)	av. (2/5)	5.19	10.8	74.1	4.36	0.46	0.205	0.100	4.34	0.244	49.2	16.6	15.6	15.9	318	235	0.28	135	309	2.38
2	std.	0.21	0.4	1.0	0.17	0.11	0.004	0.002	0.17	0.006	1.5	0.3	1.4	3.4	4	4	0.02	3	10	0.06
LNWF (geological)	av. (6/11)	5.13	10.2	74.8	4.18	0.34	0.224	0.121	4.54	0.207	39.3	12.9	50.7	12.5	269	192	1.68	120	266	1.96
6	std.	0.11	0.2	0.4	0.09	0.03	0.007	0.002	0.10	0.004	0.8	0.2	3.4	1.2	20	4	0.09	2	8	0.06
Groups 3 and 4 (LNWF)	av. (14/23)	5.23	10.7	74.1	4.27	0.41	0.217	0.115	4.45	0.198	37.8	12.8	78.1	13.7	269	191	2.28	113	246	1.93
14	std.	0.21	0.6	0.9	0.17	0.08	0.008	0.006	0.24	0.008	1.8	0.3	16.6	2.9	19	6	0.33	5	11	0.07
IC (geological)	av. (3/5)	5.20	11.9	73.7	4.40	0.43	0.192	0.100	3.72	0.175	36.0	13.2	151	13.7	214	186	4.69	104	231	1.90
3	std.	0.07	0.4	0.6	0.06	0.04	0.003	0.004	0.10	0.004	1.0	0.3	8	1.4	20	5	0.23	3	3	0.03
Group 5 (ICl)	av. (2/3)	5.13	11.6	74.2	4.27	0.39	0.191	0.097	3.73	0.181	35.4	12.8	146	11.9	222	183	4.98	105	226	1.85
2	std.	0.07	0.1	0.3	0.07	0.04	0.003	0.002	0.06	0.003	0.9	0.2	8	1.4	9	4	0.55	3	8	0.02
NIST 612	av. (1/9)	13.4	2.03	72.9	-	11.4	0.0073	0.0052	0.0043	0.0050	41.7	35.5	91.1	48.3	36.7	32.0	76.5	37.0	34.5	40.7
	std.	0.4	0.07	0.6		0.2	0.0002	0.0001	0.0026	0.0001	0.8	0.6	2.3	2.3	2.2	0.7	2.0	0.7	0.8	1.0

Table 2, cont.

Group	**Ba**	**La**	**Ce**	**Pr**	**Nd**	**Sm**	**Eu**	**Gd**	**Tb**	**Dy**	**Ho**	**Er**	**Tm**	**Yb**	**Lu**	**Hf**	**Ta**	**Th**	**U**
UNWF (geological)	2.53	180	373	36.2	138	25.9	0.99	25.2	4.05	20.4	4.00	12.0	1.56	11.1	1.56	35.6	12.6	27.0	7.47
1	0.33	0.8	10	0.7	1	0.6	0.06	2.6	0.26	0.6	0.16	0.4	0.07	0.3	0.05	0.6	0.4	0.4	0.12
Group 1 (UNWF)	2.39	176	368	35.2	138	26.1	1.07	26.8	4.29	21.0	4.03	12.5	1.58	11.5	1.56	35.9	12.8	27.1	7.65
6	0.23	5	11	0.8	3	0.9	0.19	3.0	0.33	1.4	0.18	0.8	0.08	0.7	0.06	1.3	0.7	1.4	0.53
Group 2 (UNWF)	2.03	135	297	30.0	122	26.2	0.93	27.2	4.93	25.2	4.86	15.2	1.93	14.1	1.87	43.2	16.2	33.0	10.0
2	0.08	4	9	0.7	2	0.4	0.02	1.9	0.34	0.5	0.08	0.6	0.05	0.5	0.06	1.0	0.3	0.3	0.2
LNWF (geological)	9.90	150	322	31.7	126	24.9	1.18	22.8	4.11	21.8	4.28	12.7	1.67	11.9	1.63	35.0	13.1	28.1	8.48
6	0.61	4	10	0.8	3	0.7	0.05	2.6	0.20	0.7	0.12	0.5	0.05	0.5	0.04	1.1	0.3	0.6	0.15
Groups 3 and 4 (LNWF)	13.8	137	293	29.2	117	23.6	1.07	24.0	4.17	21.1	4.10	12.7	1.62	11.7	1.57	34.3	12.7	26.8	8.13
14	2.4	9	18	1.8	8	1.4	0.11	2.2	0.33	1.1	0.19	0.7	0.07	0.6	0.07	1.6	0.5	1.0	0.27
IC (geological)	30.5	120	252	25.1	99	20.0	0.88	19.9	3.57	18.6	3.67	11.3	1.46	10.5	1.42	30.6	11.9	26.0	7.89
3	1.5	4	10	0.8	3	0.8	0.04	2.4	0.27	0.7	0.14	0.6	0.05	0.6	0.05	1.2	0.3	0.8	0.22
Group 5 (ICl)	32.5	121	256	25.4	100	20.2	0.89	20.0	3.58	18.7	3.70	11.3	1.46	10.5	1.41	31.0	11.9	26.2	7.85
2	3.6	5	11	0.5	2	0.2	0.03	0.8	0.07	0.2	0.08	0.3	0.01	0.3	0.04	0.6	0.3	0.3	0.17
NIST 612	36.5	37.2	37.8	36.0	36.0	37.7	35.0	33.9	35.6	34.3	35.9	34.9	33.6	38.1	34.2	35.5	29.9	36.0	35.6
	0.7	1.2	1.3	0.8	0.5	0.4	0.8	2.6	0.6	0.6	0.7	0.6	0.7	0.9	0.6	0.7	0.5	0.8	0.7

Table 3. Obsidian lithics collected on and in environs of Nabro volcano in 2011 and 2012.

ID	Group / source	Description	Photo 1	Photo 2
11-71E	1 / UNWF	Complete blade, which has removed neo-cortical side of core/nodule. Length 48.7 mm; maximum width 19.2 mm. Likely soft direct percussion; plain butt.		
11-51A	1 / UNWF	Partially neo-cortical flake.		
11-71C	1 / UNWF	Neo-cortical obsidian with semi-abrupt long retouch on four edges. Retouch irregular on all edges except right. Possible function as a scraping tool.		
12-04	1 / UNWF	Elongated flake. Flake with thick (6.3 mm) slightly oblique butt and bulb scar. Possibly soft percussion. Edge removals are irregular and fresher than rest of flake suggesting a second episode of use though taphonomic cause (e.g., trampling) cannot be excluded. Length: 67.0 mm; 32.2 mm at widest.		

11-71D	1 / UNWF	Small (exhausted) unipolar bladelet core with seven bladelet negatives. Heavy scarring on base and small opposing flake negatives suggests use of anvil for *débitage*, at least towards the end of core's life. Probably Neolithic		
11-38A	1 / UNWF	Neo-cortical flake with direct regular abrupt retouch on distal end and direct abrupt micro-retouch on left edge. Irregular removals along remaining edges suggestive of both retouch and taphonomy. No proximal end remaining.		
12-01	2 / UNWF	Alternating multidirectional bladelet core with three successive *débitage* surfaces. The striking platform of the second *débitage* surface was removed by the distal end of the youngest and last *débitage* surface flaked. The oldest and first *débitage* surface flaked opposes the second *débitage* surface and its striking platform is crushed likely from contact with an anvil when the second opposing *débitage* surface was flaked on anvil. Nine bladelet negatives present, the longest 45 mm. Two are hinged and may have led to abandonment of the core The last *débitage* surface demonstrates researched unipolarity and uses a previous (oldest) *débitage* surface as a striking platform. The bladelet negatives on this last surface are the most regular, but a single opposing removal suggests anvil use to stabilize the core during reduction. Neo-cortical surface remains on one face of core.		

		Direct (soft) percussion in hand and on anvil suggested. Typical of ceramic Neolithic cores found in the Afar dated to between the 3rd and 2nd millennium BCE.		
12-06	2 / UNWF	Thick neo-cortical blade flake with remains of bulb scar. No butt remaining. Edge removals irregular and fresher suggesting taphonomic causes.		
11-51G	3 / LNWF	Proximal end of blade with plain, relatively flat butt (3.0 mm thick), prominent bulb and bulb scar. Fractured distal end. Possible soft hammer percussion.		
11-51D	4 / LNWF	Partially neocortical proximal preparation flake with bulb scar.	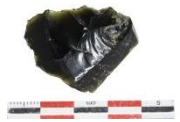	
11-51C	4 / LNWF	Medial flake.	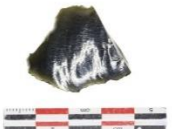	
11-51B	4 / LNWF	Neo-cortical nodule with few non-structured removals. Mostly natural.		

11-51E	4 / LNWF	Small medial flake with edge wear. Abrupt and irregular direct micro-removals on left edge.		
11-51H	4 / LNWF	Small medial flake with fine retouch along margins and plano-convex cross section.		
11-49	4 / LNWF	Triangular *pièce esquillée*. Typical tool or possibly waste of ceramic Neolithic periods in Afar and related to industries relying on bipolar on anvil flaking techniques.		
12-05	4 / LNWF	Neo-cortical plunging flake missing bulb and butt. Not used or worked. Dorsal face presents bipolar flake negatives.		
11-71B	4 / LNWF	Complete laminar blade with thin slightly oblique butt possibly removed using punch technique (suggested by morphology and angle of butt and heavy rippling) or soft hammer percussion. Length is 70.0 mm; maximum width 24.9 mm. Possibly LSA else Neolithic.		

12-07	4 / LNWF	Small blade flake. Thick slightly oblique butt with well-defined bulb. Possibly soft percussion or punch.		
11-38B	4 / LNWF	Cortical flake.		
11-71A	4 / LNWF	Complete laminar bladelet, which has removed side of core; right margin normally retouched; left margin inversely. Flatness of bulb and small size of platform suggest soft direct percussion. Length is 54.4 mm.		
12-03	4 / LNWF	Unipolar blade core with exhausted crushed platforms characteristic of bipolar flaking on anvil. All main contemporaneous blade removals are from a single direction (*n*=4), while opposing removals are (i) pre-existing negatives with slightly different patina (*n*=2) and either the result of removals from the core preparation phase or, in one case, a potential blade from an earlier blade core that was reused; (ii) small removals that are products of bipolar flaking on anvil (counter-removals) and heavily hinged negatives also characteristic of bipolar faking on anvil. Percussion on anvil was used (not pressure). Comparable to		

		ceramic Neolithic cores in Afar even though blade products are slightly larger than typical of 3rd–2nd millennium BCE. 92.2 mm from platform to platform. Maximum width: 34 mm.		
12-02	4 / LNWF	Heavily-patinated problematic core. Ridges are naturally battered, as is the non-striking platform end of the nodule, suggesting abrasion before attempted (and failed) blade *débitage* that likely included use of anvil (crushing and characteristic small opposing flakes can be seen on opposing end to striking platform). 27.4 mm longest hinged flake.		
11-51F	5 / IC	Small thick flake with abrupt direct and invasive removals on two of three edges.		
11-54	5 / IC	Distal end of a thick neo-cortical flake with indirect retouch on left edge.		

Table 4. Average compositions (and standard deviations) of archaeological obsidian samples from Yemen and Ethiopia. Elements with contents above 0.1 % are expressed in weight % of oxides, other elements are given in parts per millions of elements. Some samples were analysed multiple times to verify homogeneity. Numbers of different samples and numbers of analysis carried out are reported as follows: av. (number of samples/number of analyses).

		Na_2O	Al_2O_3	SiO_2	K_2O	CaO	TiO_2	MnO	Fe_2O_3	ZrO_2	Li	B	Mg	Sc	Zn	Rb	Sr	Y	Nb	Cs
Midaman UNWF-Group 1	av. (3/7)	5.24	11.3	73.4	4.21	0.39	0.266	0.127	4.62	0.222	52.7	11.9	26.8	20.2	264	175	0.38	111	269	1.75
	std.	0.13	0.4	0.6	0.09	0.03	0.005	0.009	0.29	0.013	3.5	0.6	3.2	3.2	19	7	0.12	9	4	0.11
Midaman UNWF-Group 2	av.(6/6)	4.94	11.3	74.2	4.08	0.32	0.215	0.102	4.31	0.254	62.7	15.7	23.3	18.2	269	213	0.29	136	325	2.30
	std.	0.13	0.3	0.4	0.10	0.02	0.004	0.002	0.11	0.005	2.7	0.5	5.7	2.7	11	6	0.05	2	4	0.08
Midaman LNWF	av.(21/22)	5.10	11.5	73.7	4.11	0.32	0.228	0.118	4.49	0.201	54.0	12.8	91.6	15.0	250	182	2.65	116	260	1.93
	std.	0.14	0.4	0.4	0.08	0.02	0.009	0.004	0.20	0.013	4.7	0.4	20.3	2.3	20	6	0.35	7	9	0.08
Midaman-Wakarida IC	av.(7/8)	5.07	12.8	73.1	4.17	0.33	0.202	0.104	3.84	0.183	47.3	13.2	156	12.9	220	177	5.37	110	243	1.93
	std.	0.18	0.3	0.5	0.10	0.05	0.008	0.002	0.11	0.010	6.7	0.3	9	5.5	11	5	0.28	6	11	0.07
DS 181	av.(2/4)	5.69	11.1	73.5	4.29	0.29	0.209	0.113	4.45	0.147	67.3	13.9	94.2	8.31	233	248	1.18	110	171	3.12
	std.	0.24	0.4	0.7	0.08	0.06	0.021	0.010	0.28	0.004	3.0	1.3	59.8	1.54	13	6	0.19	3	5	0.16

Table 4 cont.

	Ba	La	Ce	Pr	Nd	Sm	Eu	Gd	Tb	Dy	Ho	Er	Tm	Yb	Lu	Hf	Ta	Th	U
Midaman UNWF-Group 1	2.31	185	375	36.4	134	25.1	1.19	24.4	4.00	20.7	4.16	11.9	1.61	11.2	1.59	35.6	13.7	28.6	8.29
	0.24	13	18	1.8	7	1.3	0.31	2.6	0.40	1.7	0.31	1.0	0.13	0.8	0.12	1.8	0.6	1.7	0.36
Midaman UNWF-Group 2	1.87	138	300	30.5	119	26.0	0.96	24.2	4.45	25.6	5.23	14.8	2.08	14.4	2.01	44.3	18.3	35.6	10.91
	0.18	3	11	0.6	2	0.5	0.03	1.7	0.13	0.3	0.08	0.3	0.04	0.3	0.05	0.8	0.2	0.7	0.32
Midaman LNWF	14.2	138	289	30.0	116	23.6	1.13	22.6	3.81	21.8	4.43	12.4	1.76	12.1	1.70	35.5	14.4	29.0	8.82
	1.6	9	14	1.6	7	1.3	0.09	1.5	0.24	1.2	0.26	0.8	0.10	0.6	0.11	2.1	0.6	1.6	0.21
Midaman-Wakarida IC	31.7	121	252	26.3	100	20.8	0.97	20.1	3.44	20.1	4.13	11.6	1.65	11.4	1.59	32.9	13.9	28.7	8.48
	1.5	5	10	1.0	4	0.9	0.04	1.6	0.21	1.0	0.21	0.6	0.07	0.6	0.09	1.5	0.6	1.2	0.21
DS 181	6.95	140	275	25.9	95.9	19.2	1.09	18.2	3.16	19.4	4.07	12.0	1.72	12.4	1.76	26.2	9.83	31.8	7.25
	0.58	13	23	2.0	6.2	0.8	0.16	0.8	0.07	1.1	0.18	0.6	0.10	0.9	0.11	2.0	1.06	2.0	0.33